Biochemical Pharmacology 142 (2017) 229–241

Contents lists available at ScienceDirect

Biochemical Pharmacology

journal homepage: www.elsevier.com/locate/biochempharm

The neurotoxicant PCB-95 by increasing the neuronal transcriptional repressor REST down-regulates caspase-8 and increases Ripk1, Ripk3 and MLKL expression determining necroptotic neuronal death

Natascia Guida [a,1], Giusy Laudati [b,c,1], Angelo Serani [b], Luigi Mascolo [b], Pasquale Molinaro [b] Paolo Montuori [d], Gianfranco Di Renzo [b], Lorella M.T. Canzoniero [b,c], Luigi Formisano [b,c,*]

[a] IRCCS SDN, Naples 80143, Italy
[b] Division of Pharmacology, Department of Neuroscience, Reproductive and Dentistry Sciences, School of Medicine, "Federico II" University of Naples, Naples 80131, Italy
[c] Division of Pharmacology, Department of Science and Technology, University of Sannio, 82100 Benevento, Italy
[d] Department of Preventive Medical Sciences, University Federico II, Via Pansini 5, Naples 80131, Italy

ARTICLE INFO

Article history:
Received 20 April 2017
Accepted 29 June 2017
Available online 1 July 2017

Keywords:
PCB-95
REST
Necroptosis
Neuronal cell death

ABSTRACT

Our previous study showed that the environmental neurotoxicant non-dioxin-like polychlorinated biphenyl (PCB)-95 increases RE1-silencing transcription factor (REST) expression, which is related to necrosis, but not apoptosis, of neurons. Meanwhile, necroptosis is a type of a programmed necrosis that is positively regulated by receptor interacting protein kinase 1 (RIPK1), RIPK3 and mixed lineage kinase domain-like (MLKL) and negatively regulated by caspase-8. Here we evaluated whether necroptosis contributes to PCB-95-induced neuronal death through REST up-regulation. Our results demonstrated that in cortical neurons PCB-95 increased RIPK1, RIPK3, and MLKL expression and decreased caspase-8 at the gene and protein level. Furthermore, the RIPK1 inhibitor necrostatin-1 or siRNA-mediated RIPK1, RIPK3 and MLKL expression knockdown significantly reduced PCB-95-induced neuronal death. Intriguingly, PCB-95-induced increases in RIPK1, RIPK3, MLKL expression and decreases in caspase-8 expression were reversed by knockdown of REST expression with a REST-specific siRNA (siREST). Notably, *in silico* analysis of the rat genome identified a REST consensus sequence in the caspase-8 gene promoter (Casp8-RE1), but not the RIPK1, RIPK3 and MLKL promoters. Interestingly, in PCB-95-treated neurons, REST binding to the Casp8-RE1 sequence increased in parallel with a reduction in its promoter activity, whereas under the same experimental conditions, transfection of siREST or mutation of the Casp8-RE1 sequence blocked PCB-95-induced caspase-8 reduction. Since RIPK1, RIPK3 and MLKL rat genes showed no putative REST binding site, we assessed whether the transcription factor cAMP Responsive Element Binding Protein (CREB), which has a consensus sequence in all three genes, affected neuronal death. In neurons treated with PCB-95, CREB protein expression decreased in parallel with a reduction in binding to the RIPK1, RIPK3 and MLKL gene promoter sequence. Furthermore, CREB overexpression was associated with reduced promoter activity of the RIPK1, RIPK3 and MLKL genes. Collectively, these results indicate that PCB-95 was associated with REST-induced necroptotic cell death by increasing RIPK1, RIPK3 and MLKL expression and reducing caspase-8 levels. In addition, since REST is involved in several neurological disorders, therapies that block REST-induced necroptosis could be a new strategy to revert the neurodetrimental effects associated to its overexpression.

1. Introduction

Polychlorinated Biphenyls (PCBs) are organic pollutants (POPs) that persist in the environment and bioaccumulate through the food chain [1]. These toxic compounds were produced and used commercially in industrial manufacturing between the 1930s and 1970s. Although PCBs were banned in the late 1970s and early 1980s [2], these compounds can still be found in the fatty tissues of fish and marine mammals [3]. Interestingly, PCB exposure can be correlated with the development of neurological disorders, such as Alzheimer's

Abbreviations: PCBs-NDL, polychlorinated biphenyls non-dioxin-like; Nec-1, necrostatin-1; REST, repressor element-1 silencing transcription factor; CREB, CAMP Responsive Element Binding Protein; ChIP, chromatin immunoprecipitation; LDH, lactate dehydrogenase; RIPK1, receptor interacting protein kinase 1; RIPK3, receptor interacting protein kinase 1; MLKL, mixed lineage kinase domain-like; NSA, necrosulfonamide; POPs, persistent organic pollutants; ALS, amyotrophic lateral sclerosis; MS, multiple sclerosis; RE1, repressor element 1; TSS, transcription start site.

* Corresponding author at: Division of Pharmacology, Department of Science and Technology, University of Sannio, 82100 Benevento, Italy.
E-mail address: cformisa@unisannio.it (L. Formisano).
[1] Equal contribution: Natascia Guida, Giusy Laudati.

http://dx.doi.org/10.1016/j.bcp.2017.06.135
0006-2952/

[4] disease and Parkinson's disease [5], as well as amyotrophic lateral sclerosis (ALS) [6]. PCBs can be divided into two major groups: dioxin-like (DL), which have a coplanar structure, and non-dioxin-like (NDL), which adopt a non-coplanar structure [7]. *In vitro* experiments showed that both DL-and NDL-PCBs can induce apoptotic and necrotic neuronal cell death [8–10]. We previously demonstrated that the PCB mixtures Aroclor-1254 and NDL-PCB-95 both caused necrotic, but not apoptotic, neuronal death by increasing expression levels of the repressor element 1 (RE1)-silencing transcription factor (REST) [11,12]. REST represses its target genes by binding to a DNA sequence motif named the RE1 element and REST dysregulation has been associated with Alzheimer's, Parkinson's, Huntington's and Niemann-Pick type C diseases, as well as with epilepsy [13]. Furthermore, increased expression of REST, with a consequent decrease in expression of target genes, such as AMPA receptor (AMPAR) GluR2 subunit, mu opioid receptor 1 (MOR-1), miR132, cocaine- and amphetamine-regulated transcript (CART), and Na^+/Ca^{2+} exchanger 1 (NCX1), caused neuronal death [11,12,14,15]. More recently, a new type of programmed necrosis called necroptosis, has been reported [13]. Necroptosis is involved in several neurological diseases characterized by inflammation, including stroke, multiple sclerosis (MS), and ALS [16–18]. Activation of necroptosis is associated with the loss of membrane integrity, release of damage-associated molecular pattern molecules (DAMPs) and subsequent cell death [19]. Several molecular mechanisms are involved in necroptosis: (1) necroptosis stimulated when cells are deficient in caspase-8, or in the presence of a caspase inhibitor [20]; (2) activation of receptor interacting protein kinase 1 (RIPK1) as a critical upstream step event in necroptosis; (3) RIPK1 binding to RIPK3 to activate MLKL that is recruited to the plasma membrane, where it promotes pore formation and consequent cell lysis [20]. Interestingly, necroptosis can be pharmacologically reduced by the RIPK1 inhibitor necrostatin-1 (Nec-1) or its derivatives, and by the MLKL inhibitor necrosulfonamide (NSA) [21]. Since treatment with 8 μM PCB-95 for 24 h could induce necrotic neuronal death in a caspase-independent manner [11] that involved REST, in this study we investigated whether necroptosis is implicated in the neurotoxic effect of PCB-95 by examining whether Nec-1 can modulate PCB-95-induced cell death and if PCB-95 treatment affects REST-mediated regulation of gene and protein expression of RIPK1, RIPK3, MLKL and caspase-8.

2. Material and methods

2.1. Materials

The compound 2,3,6-2′,5′-pentachlorinated biphenyl (PCB-95) (cod: RPC-130AS) (stock solution 305 μM) was purchased from Ultra Scientific (North Kingstown, RI, USA). Culture media and sera were purchased from Invitrogen (Milan, Italy). The RIPK1-inhibitor 5-(Indol-3-ylmethyl)-3-methyl-2-thio-Hydantoin, Necrostatin-1 (Nec-1) was purchased from Sigma (Milan, Italy) (cod. N9037; stock solution 20mM), For those requiring dilution in Dimethyl sulfoxide (DMSO), the final DMSO concentration was 0.1% that did not induce cellular toxicity. All restriction enzymes, DNA-modifying enzymes and Luciferase reporter kits were purchased from Promega Italy. Synthetic oligonucleotides were from Eurofins Genomics. All siRNAs used were purchased from Quiagen Italy. siRNAs for RIPK1 (siRIPK1) (SI01685873), RIPK3 (siRIPK3) (SI02026409), MLKL (siMLKL) (SI03308753), whereas for REST (siREST) and negative control (siCTL) have been already published [22].

2.2. Cell Cultures and drug treatment

SH-SY5Y human neuroblastoma cells at passages 15–20 and cortical neurons (DIV 7–9) from rat embryos were prepared as previously reported [22,23]. All the experiments on primary cortical neurons were performed according to the procedures described in experimental protocols approved by the Ethics Committee of the 'Federico II' University of Naples. PCB-95 treatment was performed in low serum. For Nec-1 experiments neurons were pre-treated for 2 h with the drug at 1, 5, 10 and 20 μM followed with PCB-95 8 μM for 24 h. The plates used and the density of cells plated have been previously published [22].

2.3. Cloning of the caspase-8, RIPK1, RIPK3 and MLKL promoter regions

Approximately 1-Kb fragments, including the putative rat caspase-8, RIPK1, RIPK3 and MLKL promoter sequences were found by Genomatix software (http://genomatix.de). Amplification of these promoter regions was performed using PrimeSTAR GLX Pfu DNA polymerase (cod: R050A: Takara) on rat genomic DNA. Caspase-8 amplicon primers from base −1216 (5-CAAATGCACA GAACAGCTGATTATACC-3) to base +15 (5-CGCCCGCCAGTTC TTAAGG-3) of exon 1 (Ensembl association number: ENSRNOE00000313891). RIPK1 amplicon primers from base −824 (5-CTGTGAATGTTTGGGATTTGGAGG-3) to base +22 (5-CGGTCCCCAGCTCTGAAA-3) of exon 1 (Ensembl association number ENSRNOE00000455609). RIPK3 amplicon primers from base −1387 (5-CTTTTCTGAGACAGGAAGCACGG-3) to base +18 (5-GGCTCAGCTTGGGTCTCTG-3) of exon 1 (Ensembl association number ENSRNOE00000199113). MLKL amplicon primers from base −1174 (5-GCTGGAGAGATGGCTTAGTGG-3) to base +26 (5-GAT GATCTGTCCCAATTTATCCATACC-3) of exon 1 (Ensembl association number ENSRNOE00000223514). The amplified fragments were cloned in the pSC-B vector using the StrataClone Blunt PCR Cloning Kit (cod: 240207, Agilent Technologies, USA) and their identities were confirmed by DNA sequence analysis. The Caspase-8, RIPK1, RIPK3 and MLKL fragments containing the putative promoter regions were subcloned upstream of the firefly luciferase open reading frame in the pGL3basic vector by using Not1 and Xho1 restriction enzymes. These new constructs were named pGL3-casp8, pGL3-RIPK1, pGL3-RIPK3 and pGL3-MLKL. Presumed REST binding site on Caspase-8 promoter and presumed CREB binding sites on RIPK1, RIPK3 and MLKL promoters were predicted by using Jaspar database [24]. Mutagenesis of REST binding site on Caspase-8 and CREB binding sites on RIPK1, RIPK3 and MLKL was performed by Quik Change Site-Directed Mutagenesis Kit (cod:200518, Stratagene, USA) to obtain the following constructs: (1) pGL3-casp8-RE1mut (GTGCTGTCCAGGGTGCTGT), (2) pGL3-RIPK1-CRE-mut (GTGTATTTGACATCAAATT), (3) pGL3-RIPK3-CRE-mut (TTTCTG GTGAGGTACATTTTC) and (4) pGL3-MLKL-CRE-mut (TCTGTAATGAGGTCTGATGCC), in which underlined bases represent mutated sequences.

2.4. Small Interfering RNAs (siRNAs), constructs transfections

siRNAs and constructs transfections in neurons were performed 24 h before PCB-95 exposure with Lipofectamine LTX (15338–100, Invitrogen, Milan, Italy), in accordance with the manufacturer's protocol, as previously reported [11]. Specifically, siRIPK1, siRIPK3 and siMLKL were transfected at the concentration of 50nM, whereas siREST and siCTL as previously published [11]. For CREB overexpression, cortical neurons were transfected with 15 μg of construct RSV CREB, that was a gift from Marc Montminy (Plasmid # 22394 Addgene, Teddington, UK) [25], or with the empty vector pRC/RSV (Mock). For ChIP assay experiments on exogenous chromatin in SH-SY5Y, cells were transiently transfected, as previously described [22], with the following constructs:pGL3-casp8 or pGL3-casp8-RE1mut, pGL3-RIPK1 or pGL3-RIPK1-CREmut, pGL3-RIPK3

or pGL3-RIPK3-CREmut and pGL3-MLKL or pGL3-MLKL-CREmut. After 6 h of incubation with transfection mix the medium was changed with DMEM containing PCB-95 8 μM and left for 24 h. Transfection efficiency was approximately of about 45% for SH-SY5Y cells and 35% for cortical neurons (data not shown).

2.5. Luciferase assay experiments

To study the Caspase-8, RIPK1, RIPK3 and MLKL promoter activities, cortical neurons were co-transfected with 1,5 μg of total DNA constructs, including 800 ng of reporter vectors, that are: for Caspase-8 experiments (1) pGL3basic, (2) pGL3-casp8, (3) pGL3-casp8-RE1mut; for RIPK1 experiments: (1) pGL3basic, (2) pGL3-RIPK1, (3) pGL3-RIPK1-CREmut; for RIPK3 experiments: (1) pGL3basic, (2) pGL3-RIPK3, (3) pGL3-RIPK3-CREmut; for MLKL experiments: (1) pGL3basic, (2) pGL3-MLKL, (3) pGL3-MLKL-CREmut. For siRNAs transfection, 50 nM of siCTL or siREST was used. To overexpress CREB, we co-transfected 500 ng of CREB construct or empty vector. In all luciferase experiments each transfection mix contained 200 ng of the pRL-TK vector expressing the renilla luciferase gene, that provides an internal control value to which expression of the firefly luciferase reporter gene has been normalized. After 2 h of incubation with transfection mix the medium was replaced with a fresh one containing PCB-95 (8 μM) and analyzed after 24 h with the Dual-Luciferase Reporter Assay System kit (E1910) (Promega Italy). Luciferase activity was expressed as firefly-to-renilla ratio.

2.6. qRT-PCR analysis

First-strand cDNA, qRT-PCR and data analysis were performed as previously published [26]. qRT-PCR was performed in a 7500 Fast real-time PCR system. Protocol for the amplification was previously described [27]. The data were normalized by hypoxanthine phosphoribosyl-transferase (HPRT) as an internal control. Differences in mRNA content between groups were calculated as normalized values by using 2^{-DDct} formula. The oligonucleotide sequences were: for Caspase-8 (FW 5′-GATCATGGACTGGGACGAGT TAA-3′ 2376–2398 and RV 5′-CCAGAATCGCATGCAGACAA-3′ 2436–2417) (GenBank accession number XM_008767135.2), for RIPK1 (FW 5′-GCATGACTGTGTGCCCTTACC-3′ 1324–1344 and RV 5′-CAGC GAACCGGGTTGTTCT-3′ 1381–1363) (GenBank accession number NM_001107350.1), for RIPK3 (FW 5′-CAAAAAGGTACAGAGGTG GATTGC-3′ 1425–1486 and RV 5′-GGCGGTCCAGCATTTCAT-3′ 1466–1483) (GenBank accession number NM_139342.1), for MLKL (FW 5′-AATGCTCACTAAAACCCATGCA-3′ 871–892 and RV 5′-CCTT CGGAATCTCCTTGACTTG-3′ 912–933) (GenBank accession number XM_008772570.2) and for CREB (FW 5′-TTGCCACATTAGCCCAGG TAT-3′ 353–373 and RV 5′-ACCTGGACTGTCTGCCCATT-3′ 433–452) (GenBank accession number XM_017596652.1). Data are obtained from three independent experiments.

2.7. Western blotting analysis and immunoprecipitation

Neurons were collected in ice-cold lysis buffer[28] containing anti-protease mixture (P8340 Sigma). Loaded proteins were 200 μg for Caspase-8, 120 μg for RIPK1 and 50 μg for RIPK3 and MLKL, and all were separated on 8% SDS polyacrylamide gels. CREB (60 μg) was separated on 10% SDS polyacrylamide gels. Immunoprecipitation of MLKL was performed as previously described [28]. The precipitated samples were then subjected to Western blot analysis as previously described [11,28]. The membranes were incubated overnight at 4 °C in the blocking buffer with polyclonal antibodies against REST [29], Caspase-8 (sc-6136, Santa Cruz Biotechnology, CA, USA), RIPK1 (sc-41169, Santa Cruz Biotechnology), RIPK3 (sc-135170, Santa Cruz Biotechnology), and MLKL (orb229539, Biorbyt, Cambridge, UK) at 1:500 dilution, 1:1000 monoclonal antibody for CREB (sc-271 Santa Cruz Biotechnology) and for β-Actin (A4700 Sigma) and 1:5000 monoclonal antibody for Tubulin (T5168 Sigma). In all the experiments the optical density of the bands was normalized to β-Actin or Tubulin. Data are obtained from three independent experiments.

2.8. Chromatin immunoprecipitation (ChIP) assays

ChIP assays were performed with cortical neurons with or without PCB-95 and by using 3 μg of antibody for REST [22] or for CREB and polyclonal IgG as negative control [22]. Two-microliter aliquots of immunoprecipitated DNA (in duplicate for each treatment group) were amplified by PCR with Fast SYBR green master mix (Applied Biosystems) in a 7500 Fast real-time PCR system Protocol. The primers used for amplification of immunoprecipitated DNA were for Caspase-8:FW 5′-TTCCAGACCGAGACCCAGAA-3 (ChIP-casp8), RV 5′-TGAGCAATTAAAGAACAGGGTCAA-3′; for RIPK1: FW 5′-TTGGAGGCTTTTTATGTGTATTTGAC-3′ (ChIP-RIPK1), RV 5′-T CGGTCCCCAGCTCTGAAA-3′; for RIPK3: FW 5′-TTGGCTTGTTTTTCC TTTGTTTG-3′ (ChIP-RIPK3), RV 5′-CTCACCAGAAAGGGAGAAA TATCC-3′; and for MLKL: FW 5′-AATGAGGTCTGATGCCCTCTTC-3′ (ChIP-MLKL), RV 5′-GCATCCTTTCAATTTCTGTGACTTT-3′. Results obtained from three different PCR experiments were expressed as a percentage of the control, all normalized for the DNA input.

2.9. Transient transfection ChIP

For the transient ChIP assay, SH-SY5Y cells at 50% of confluence were transfected for Caspase-8 experiments with: (1) pGL3-casp8, (2) pGL3-casp8-RE1mut; for RIPK1 experiments with: (1) pGL3-RIPK1, (2) pGL3-RIPK1-CREmut; for RIPK3 experiments with: (1) pGL3-RIPK3, (2) pGL3-RIPK3-CREmut; for MLKL experiments with: (1) pGL3-MLKL1, (2) pGL3-MLKL-CREmut. 24 h after transfection, cells were exposed to PCB-95 (8 μM/24 h). Transfection conditions and ChIP assay have been performed as described above. Antibodies used in the procedure include anti-REST, anti-CREB, and polyclonal IgG as negative control. Exogenous DNA containing: (1) pGL3-casp8 or the mutated pGL3-casp8-RE1mut was amplified using as forward primer ChIP-casp8; (2) pGL3-RIPK1 or the mutated pGL3-RIPK1-CREmut was amplified using as forward primer ChIP-RIPK1; (3) pGL3-RIPK3 or the mutated pGL3-RIPK3-CREmut was amplified using as forward primer ChIP-RIPK3; (4) pGL3-MLKL or the mutated pGL3-MLKL-CREmut was amplified using as forward primer ChIP-MLKL. For all PCR experiments of transient transfection ChIP assay LucNrev was used as reverse primer [22]. Results were expressed as the percentage of the pGL3-casp8 or pGL3-RIPK1 or pGL3-RIPK3 or pGL3-MLKL and all were normalized to their respective DNA input. Results obtained from three different PCR experiments were expressed as a percentage of the control, all normalized for the DNA input.

2.10. Determination of cell death

Cell injury was assessed with the lactate dehydrogenase (LDH) cytotoxicity kit from Cayman, as previously reported [14].Cortical neurons had been treated with PCB-95 8 μM for 24 h alone or after: (1) 2 h pretreatment with Nec-1 at 1, 5, 10 and 20 μM, or (2) transfection with siCTL, siRIPK1, siRIPK3 and siMLKL. Neurons treated with 1% Triton X-100 (Sigma) was considered 100% of cell death. Data are obtained from three independent experiments.

2.11. Statistical analysis

Data are expressed as mean ± SEM. Statistical analysis was performed with GraphPad Prism 5.0 (La Jolla, CA, USA). For the analy-

sis among more than two experimental conditions one-way ANOVA with Tukey's post hoc test was used, whereas for the analysis between two experimental groups unpaired Student's *t* test was used. $^{*}P \leq 0.05$ was considered statistically significant.

3. Results

3.1. PCB-95 induces an increase in RIPK1, RIPK3 and MLKL expression and interaction in cortical neurons

Exposure to 8 μM PCB-95 for 12 and 24 h induced a significant increase in the mRNA and protein expression of the positive regulators of necroptosis RIPK1, RIPK3 and MLKL, whereas that of the negative regulator of necroptosis [16] caspase-8 was reduced compared to the control (Fig. 1A–E). Since RIPK1-RIPK3-MLKL form a complex termed the necrosome, which is a marker of cell death [30], we investigated RIPK1-RIPK3-MLKL interactions in neurons exposed to PCB-95. Immunoprecipitation of neuronal cell lysates with an anti-MLKL antibody demonstrated an increase in RIPK1-RIPK3-MLKL interactions after PCB-95 exposure, relative to control neurons (Fig. 1F). Together these results indicated that PCB-95 exposure can affect levels and interactions of proteins involved in necrosome formation.

3.2. Nec-1 treatment or RIPK1, RIPK3 and MLKL knocking-down reduce PCB-95-induced cell death

LDH assays indicated that neuronal survival significantly improved in a dose-dependent manner when neurons were pretreated with increasing amounts of Nec-1 (1, 5, 10 and 20 μM), as compared to cells exposed to PCB-95 alone. Nec-1 yielded maximum neuroprotection at 10 μM (Fig. 2A). To evaluate the role of RIPK1, RIPK3 and MLKL in modulating PCB-95-induced cell death, neurons were transfected with siRIPK1, siRIPK3 and siMLKL, which reduced protein expression by 42%, 39%, and 37%, respectively, compared to transfection with non-specific control siRNA, siCTL (Fig. 2B–D). Importantly, as revealed by LDH release, PCB-95-induced neuronal death was significantly reduced following RIPK1, RIPK3 and MLKL expression knockdown (Fig. 2E).

3.3. REST knockdown prevents RIPK1, RIPK3, MLKL up-regulation and caspase-8 down-regulation in neurons exposed to PCB-95

Because REST is involved in PCB-95 induced neuronal death mechanisms [11], we evaluated the effect of siREST transfection on RIPK1, RIPK3, MLKL and caspase-8 expression in PCB-95-treated neurons. siREST efficiency to reduce REST protein expression was already published [11].

Notably, siREST transfection significantly blocked PCB-95-mediated increases in RIPK1, RIPK3, MLKL gene and protein expression (Fig. 3A–C, E–G), and reverted PCB-95-dependent reductions in caspase-8 gene and protein expression (Fig. 3D, H). Together these results suggest that REST has a role in necroptosis regulated by the RIPK1-RIPK3-MLKL-Casp8 pathway.

3.4. PCB-95 reduces caspase-8 promoter activity by binding to a specific RE1 sequence

By a search of the Jaspar database [31] (www.jaspar.genereg.net) with a search threshold score of 90.0, we found an RE1 element in the genomic region upstream of rat caspase-8-coding sequence (ENSRNOE00000313891), named Casp8-RE1, that was located on the forward DNA strand from nucleotides −1153 to −1134 relative to the transcription start site (TSS) (Fig. 4A, B). ChIP analysis demonstrated that REST binding to the caspase-8 promoter significantly increased after PCB-95 exposure (Fig. 4C). To corroborate the specific action of REST on the caspase-8 gene, we generated two reporter vectors containing the caspase-8 promoter region (−1216/+15): the first carried the wild type rat Casp8-RE1 site (pGL3-casp8) and the second had a mutation in the RE1 element (pGL3-casp8-RE1mut). Transfection of these vectors in neurons demonstrated that PCB-95-mediated decreases in pGL3-casp8 promoter activity were completely blocked when cells were transfected with the pGL3-casp8-RE1mut construct or by siREST transfection (Fig. 4D). To confirm that REST binds the Casp8-RE1 sequence, SH-SY5Y cells were transfected with pGL3-casp8 or pGL3-casp8-RE1mut and treated or not with PCB-95. As expected, exposure of cells to 8 μM PCB-95 for 24 h increased REST expression in SH-SY5Y cells. Meanwhile, PCB-95 treatment increased REST binding to caspase-8 exogenous promoter sequences in cells transfected with the pGL3-casp8 construct compared to untreated neurons (Fig. 4E), whereas cells transfected with pGL3-casp8-RE1mut had diminished REST binding to exogenous caspase-8 promoter sequence compared with cells transfected with pGL3-casp8 in the presence of PCB-95.

3.5. PCB-95 induces REST-dependent reductions in CREB to increase RIPK1, RIPK3 and MLKL mRNA and protein expression

Since a Jaspar search (threshold score of 90.0) showed no RE1 sites in the genomic regions upstream of the coding sequences for RIPK1 (ENSRNOE00000455609), RIPK3 (ENSRNOE00000199113) and MLKL genes (ENSRNOE00000223514), and because PCB-95 regulates the transcription factor CREB expression in neurons [32], we searched for potential CRE sites in the above-mentioned genomic regions. Interestingly, one putative CREB binding sequence in each of the genomic regions upstream of the RIPK1, RIPK3, and MLKL gene coding sequences was identified (Fig. 5A–D), indicating that transcription of these genes may be directly regulated by CREB. We named these sequences RIPK1-CRE, RIPK3-CRE and MLKL-CRE, which are located on the forward DNA strand from nucleotides −792 to −771, −1013 to −992 and −1081 to −1060, respectively, relative to the transcription start site (TSS).

Jaspar database searches (threshold score of 90.0) of genomic regions upstream of the coding sequences of CREB in the rat genome (ENSRNT00000018326.5; Chr 9: 71228108–71230488 (−2000 to +350) were analyzed to identify a putative RE1 site. Notably, no REST binding site was found (data not shown). Next, we evaluated the effect of siREST on CREB expression in PCB-95-treated cells. As shown in Fig. 6A, B, siREST transfection significantly reverted PCB-95-reduced CREB protein expression, whereas CREB mRNA levels were unaffected by either PCB-95 exposure alone or in combination with siREST. Therefore, to characterize how CREB determines increases in RIPK1, RIPK3 and MLKL gene and protein expression following PCB-95 exposure, PCB-95-treated neurons were transfected with a construct to overexpress CREB, which increased CREB protein levels by 63% (Fig. 6C). Interestingly, CREB overexpression significantly reverted PCB-95-mediated increases in RIPK1, RIPK3 and MLKL mRNA and protein expression (Fig. 6D–I).

3.6. PCB-95 decreases CREB binding to RIPK1, RIPK3 and MLKL promoter sequences resulting in increased promoter activity

PCB-95-treated neurons had significantly reduced CREB binding to RIPK1-CRE, RIPK3-CRE and MLKL-CRE sites compared to control cells (Fig. 7A, D, G). To study the role of PCB-95-mediated reductions in CREB expression to modulate RIPK1, RIPK3 and MLKL transcription, we inserted a ∼1.000 bp DNA fragment upstream of the putative TSS for RIPK1, RIPK3 and MLKL genes carried in pGL3-based vectors to generate three reporter constructs for luciferase

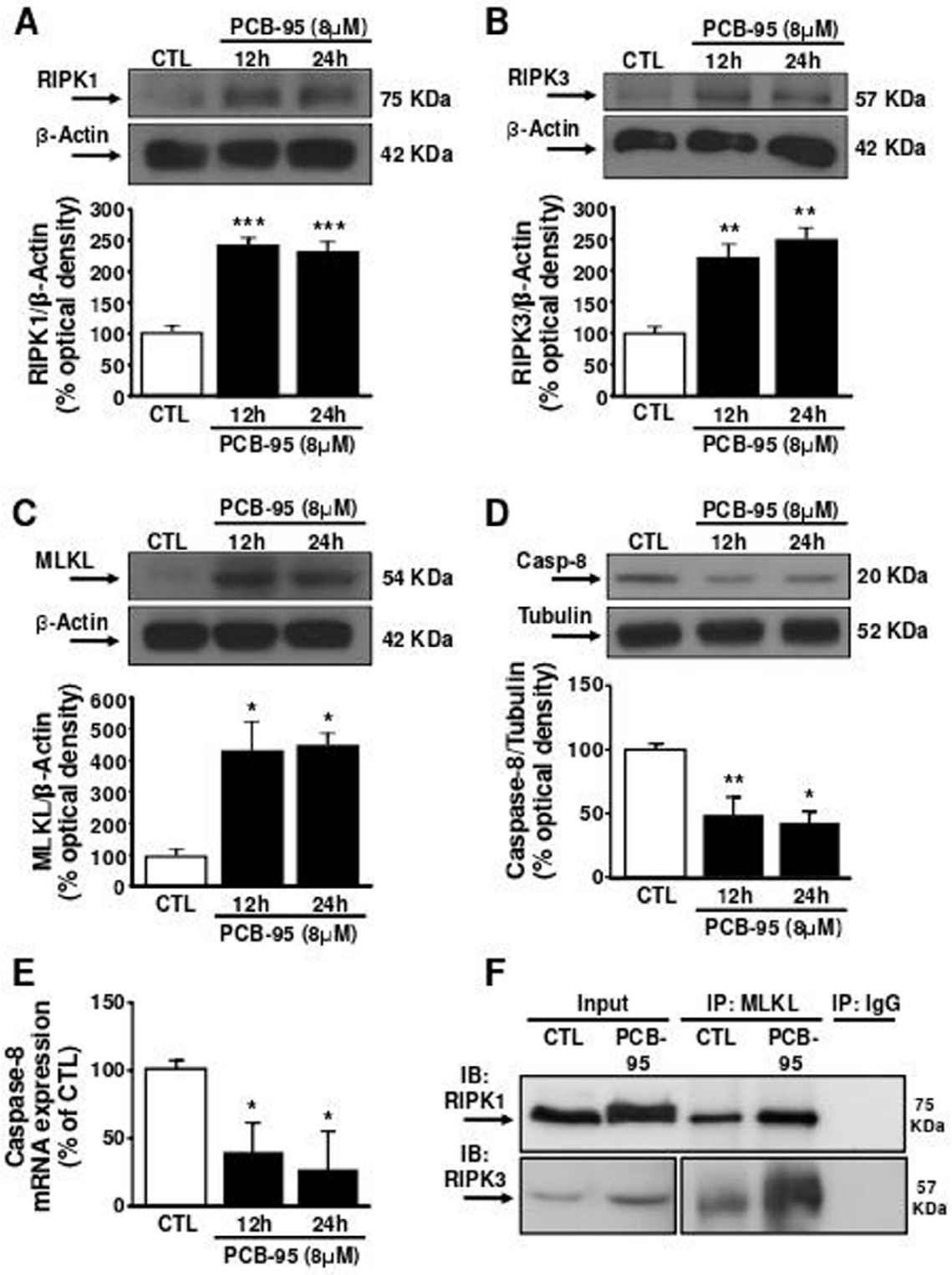

Fig. 1. Effect of 12 and 24 h of PCB-95 on RIPK1, RIPK3, MLKL protein expression and caspase-8 mRNA and protein expression. (A-D) Western blots of RIPK1, RIPK3, MLKL, Caspase-8 in cortical neurons treated for 12 and 24 h with PCB-95 (8 μM). Bars represent the mean ± S.E.M. obtained from three independent experiments. Asterisk symbols on columns indicate differences between Control (CTL) and PCB-95 treatment. $^{*}p \leq 0.05$, $^{**}p \leq 0.01$, $^{***}p \leq 0.001$ (one-way ANOVA with Tukey's post hoc test). (E) qRT-PCR of caspase-8 in cortical neurons treated for 12 and 24 h with PCB-95 (8 μM). Graphs show quantification of ratio of caspase-8 to HPRT. Bars represent mean ± S.E.M. obtained from three independent experiments. Asterisk symbols on columns indicate differences between Control (CTL) and PCB-95 treatment. $^{*}p \leq 0.05$ (one-way ANOVA with Tukey's post hoc test). (F) Representative Western blot showing immunoprecipitation between MLKL and RIPK1, and between MLKL and RIPK3 after 24 h of 8 μM PCB-95 treatment. IgG was used as a negative control.

assays: pGL3-RIPK1, pGL3-RIPK3 and pGL3-MLKL. Notably, the promoter activity in neurons transfected with pGL3-RIPK1, pGL3-RIPK3 and pGL3-MLKL strongly increased after PCB-95 treatment, whereas co-transfection of a plasmid overexpressing CREB counteracted these PCB-95-dependent increases (Fig. 7B, E, H). In addition, transfection of neurons with constructs carrying mutated

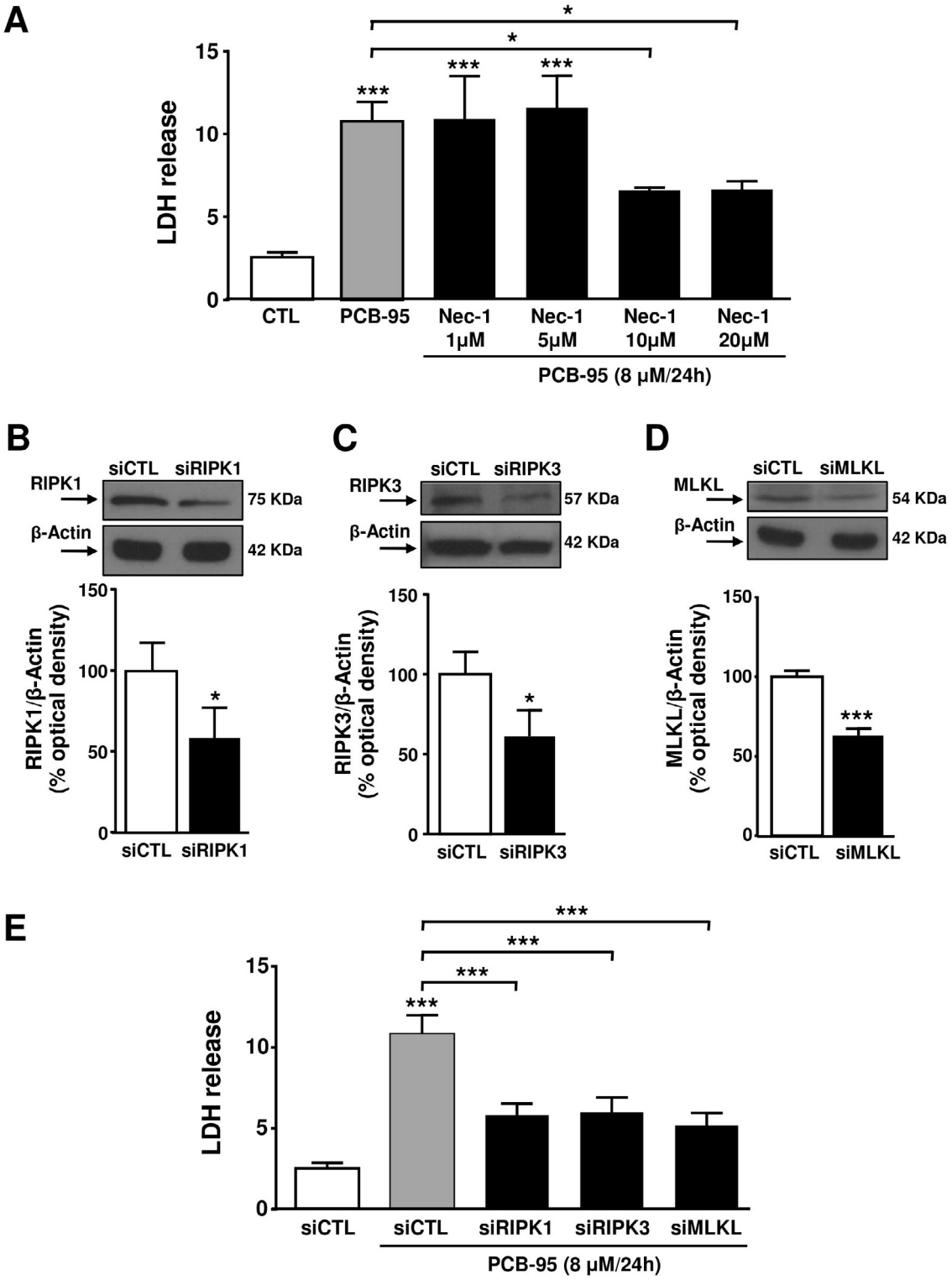

Fig. 2. Effect of Necrostatin-1 and siRIPK1, siRIPK3 and siMLKL on PCB-95-induced neuronal death. (A) LDH release in neurons pre-treated for 2 h with Nec-1 at 1, 5, 10 and 20 μM and with PCB-95.Asterisk symbols on columns indicate the significance compared with CTL and asterisk symbols on brackets indicate differences between PCB-95 and PCB-95 + Nec-1 10 and 20 μM. $^{*}p \leq 0.05$, $^{***}p \leq 0.001$ (one-way ANOVA with Tukey's post hoc test).(B-D) Western blots of RIPK1, RIPK3, MLKL in neurons transfected with siRIPK1, siRIPK3, siMLKL or siCTL. Bars represent the mean ± S.E.M. obtained from three independent experiments. $^{*}p \leq 0.05$, $^{***}p \leq 0.001$ vs siCTL (unpaired *t* test). (E) LDH release in neurons transfected with siCTL, siRIPK1, siRIPK3 and siMLKL and treated with PCB-95. Asterisk symbols on columns indicate differences between siCTL and PCB-95 + siCTL; asterisk symbols on brackets indicate differences between siCTL + PCB-95 and PCB-95 with siRIPK1, siRIPK3, siMLKL. $^{***}p \leq 0.001$ (one-way ANOVA with Tukey's post hoc test).

putative CRE sites (pGL3-RIPK1-CREmut, pGL3-RIPK3-CREmut and pGL3-MLKL-CREmut) resulted in a significant increase in promoter activity compared to cells transfected with wild type constructs (pGL3-RIPK1, pGL3-RIPK3 and pGL3-MLKL; Fig. 7B, E, H).

To validate that CREB binds in a sequence-specific manner to RIPK1, RIPK3 and MLKL promoter sequences, SH-SY5Y with or without PCB-95 treatment were transfected with pGL3-RIPK1, pGL3-RIPK3, pGL3-MLKL, or with pGL3-RIPK1-CREmut, pGL3-

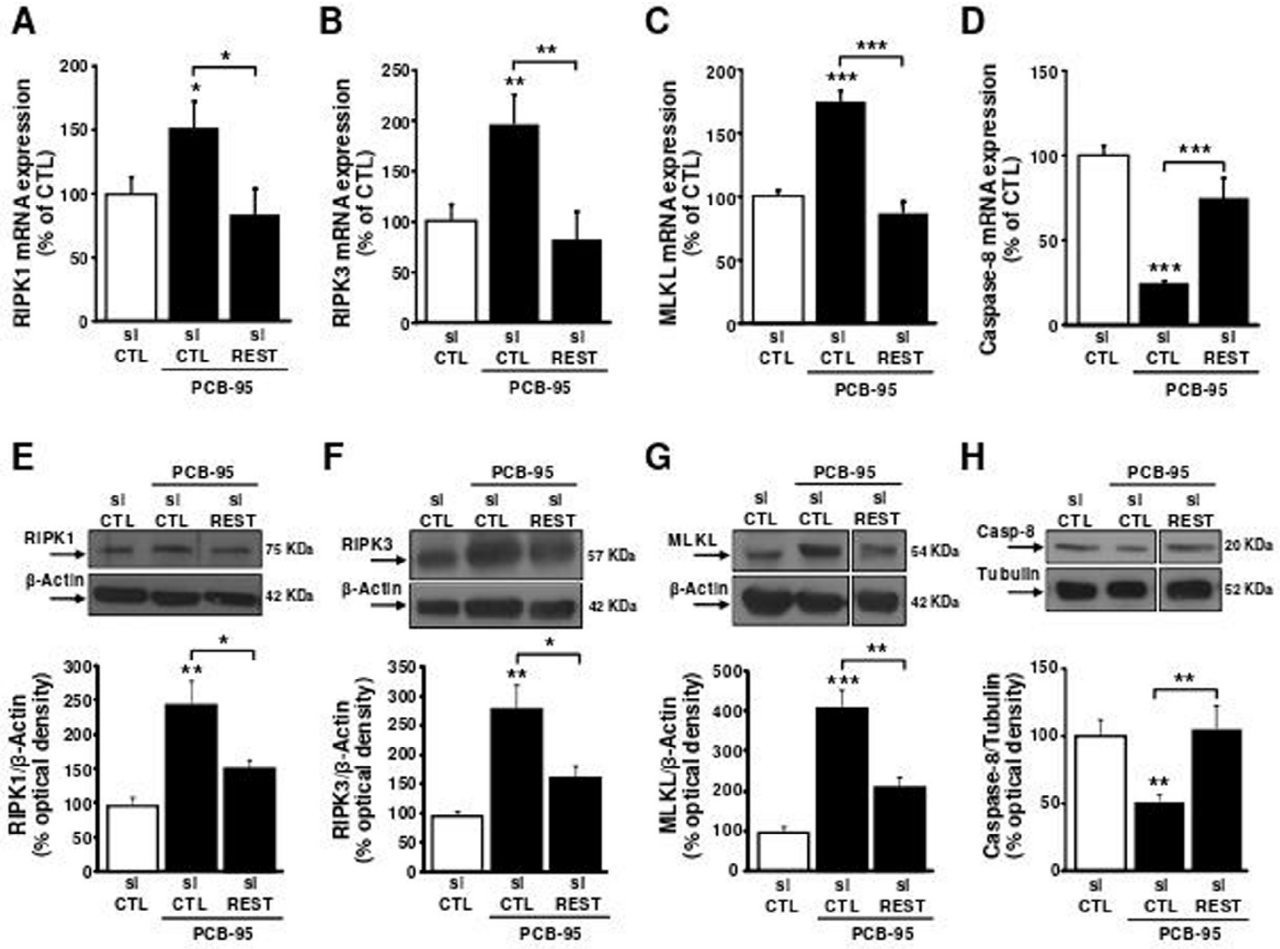

Fig. 3. Effect of siREST on RIPK1, RIPK3, MLKL and caspase-8 gene and protein expression in PCB-95-treated neurons. (A–D) qRT-PCR of RIPK1, RIPK3, MLKL and caspase-8 in cortical neurons treated with 8 μM of PCB-95 for 24 h and transfected with siCTL or siREST. Graphs show quantification of ratio of RIPK1, RIPK3, MLKL and Caspase-8 to HPRT. Bars represent mean ± S.E.M. obtained from three independent experiments. (E–H) Western blotting of RIPK1, RIPK3, MLKL and Caspase-8 in neurons treated with 8 μM of PCB-95 for 24 h and transfected with siCTL or siREST. Asterisk symbols on columns indicate differences between siCTL and siCTL + PCB-95. Asterisk symbols on brackets indicate differences between siCTL + PCB-95 and siREST + PCB-95. $^{*}p \leq 0.05$, $^{**}p \leq 0.01$, $^{***}p \leq 0.001$ (one-way ANOVA with Tukey's post hoc test).

RIPK3-CREmut and pGL3-MLKL-CREmut. Notably, SH-SY5Y cells treated with 8 μM PCB-95 for 24 h had significantly reduced CREB protein expression (data not shown). Moreover, PCB-95 treatment reduced CREB binding to RIPK1, RIPK3 and MLKL exogenous promoter sequences, whereas transfection of vectors containing a mutation in the CRE sites reverted this effect. These results suggest that PCB-95 increased RIPK1, RIPK3 and MLKL gene transcription via CREB down-regulation (Fig. 7C, F, I).

4. Discussion

This study demonstrated that neuronal cell death induced by PCB-95 involves activation of the necroptotic pathway. Interestingly, we found that PCB-95 exposure modifies the expression of genes and proteins that are reported to be important for necroptosis. PCB-95 treatment caused an increase in RIPK1, RIPK3 and MLKL gene and protein expression, as well as increased amounts of protein interactions, in parallel with a reduction in the expression of the known necroptosis regulator, caspase-8 [16]. Furthermore, treatment with the RIPK1 inhibitor Nec-1 or transfection with siRNAs against RIPK1, RIPK3 and MLKL reduced PCB-95 neurotoxicity. PCB-95-dependent changes in RIPK1, RIPK3, MLKL and caspase-8 expression likely occurred through up-regulation of the transcriptional repressor REST, which was previously shown to be involved in PCB-induced neuronal death [11,12,14,15]. Mechanistically, we found that REST binding to an RE1 site in the rat caspase-8 promoter, Casp8-RE1, down-regulated caspase-8 expression, whereas reductions in CREB expression and its consequent binding to CRE sites on RIPK1, RIPK3 and MLKL rat gene promoter sequences increased expression of these genes. To our knowledge, this report is the first to show that in neurons: (1) caspase-8 is a REST target gene, (2) RIPK1, RIPK3 and MLKL are CREB target genes, and (3) PCB-95 induced cell death by a necroptosis mechanism. The casp-8-RE1 site present in the caspase-8 gene is located on the forward DNA strand, specifically between nucleotides −1153 to −1134 from the TSS. REST binding to the Casp8-RE1 site is selective, as revealed by ChIP experiments. In fact, site directed mutagenesis of the Casp8-RE1 sequence in neurons completely abolished PCB-95-induced reductions in caspase-8 transcription due to a reduction in REST binding to its promoter sequence, as revealed by ChIP assay with a REST antibody in SH-SY5Y cells transiently transfected with pGL3-casp8 or pGL3-casp8-RE1-mut. Furthermore, PCB-95-induced REST up-regulation diminished caspase-8 protein expression in neurons. These results are consistent with previous work showing that transfection with the vector REST−VP16, in which the REST/NRSF repressor domains were replaced with the activation domain of viral protein (VP16), increased caspase-8 activity.

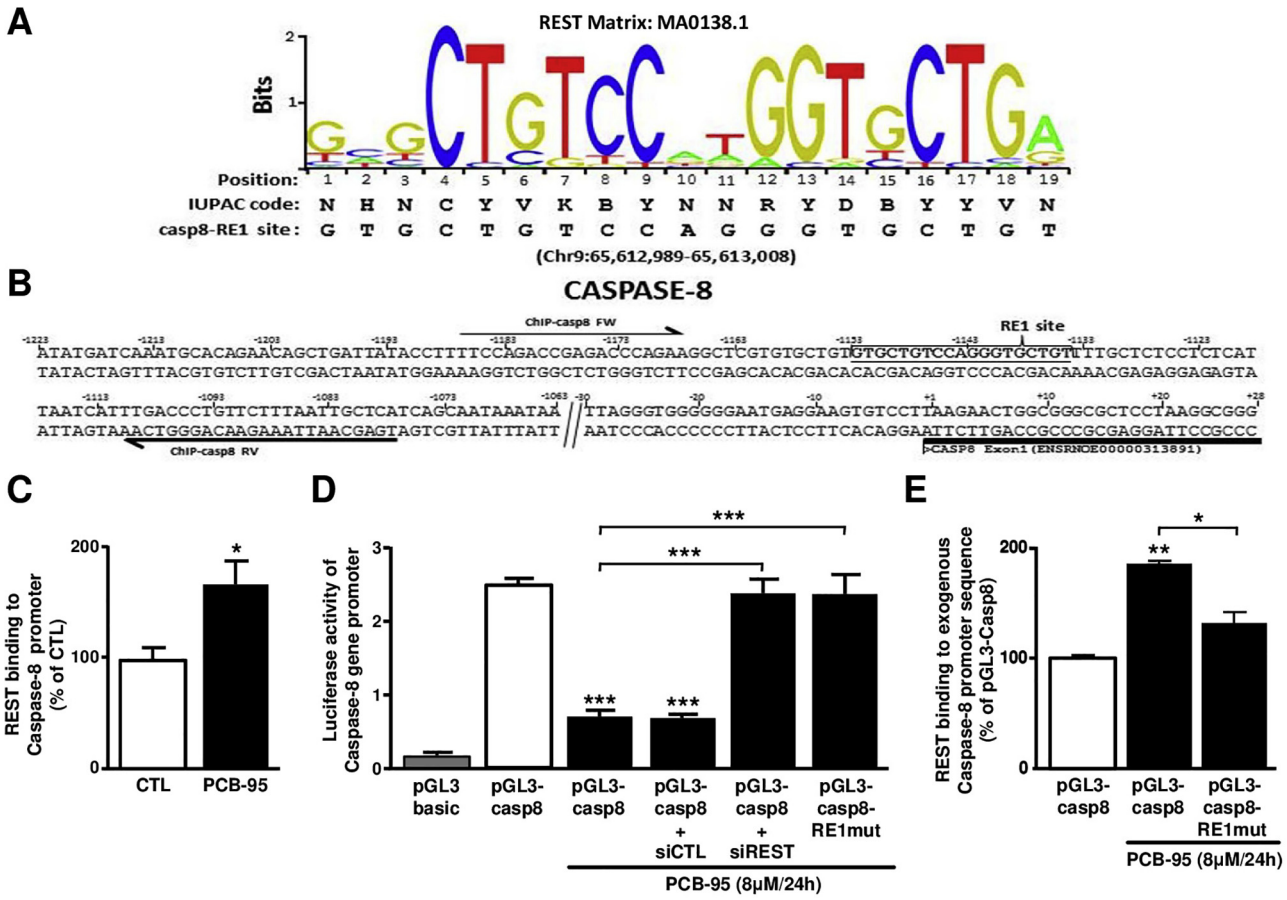

Fig. 4. REST represses caspase-8 rat gene by direct binding to an RE1 site on its promoter region. (A) JASPAR matrix representation (MA0138.1) of the consensus REST binding site on rat caspase-8 gene (casp8-RE1). casp8-RE1 sequence is represented in IUPAC code. (B) Partial sequence of the genomic caspase-8 region upstream of the exon-1 containing the underlined predicted REST binding site. (C) ChIP with anti-REST of the region containing the RE1 binding site on the caspase-8 gene promoter in PCB-95-treated neurons (8 μM/24 h). Bars represent the mean ± S.E.M. obtained from three independent experiments. $^{*}p \leq 0.05$ vs CTL (unpaired *t*-test). (D) Luciferase assay in neurons under the following experimental conditions: (1) pGL3basic, (2) pGL3-casp8, (3) pGL3-casp8 + PCB-95, (4) pGL3-casp8 + siCTL + PCB-95, (5) pGL3-casp8 + siREST + PCB-95, (6) pGL3-casp8-RE1mut + PCB-95. Bars represent the mean ± S.E.M. obtained from three independent experiments. Asterisk symbols on columns indicate differences vs pGL3-casp8; asterisk symbols on brackets indicate differences between pGL3-casp8 + PCB-95 and pGL3-casp8 + siREST + PCB-95 or pGL3-casp8-RE1mut + PCB-95. $^{***}p \leq 0.001$ (one-way ANOVA with Tukey's post hoc test). (E) Chromatin was immunoprecipitated with anti-REST from SH-SY5Y cells transiently transfected with pGL3-casp8 and pGL3-casp8-RE1mut and exposed to PCB-95. Asterisk symbols on columns indicate differences vs pGL3-casp8; asterisk symbols on brackets indicate differences vs pGL3-casp8 + PCB-95. $^{*}p \leq 0.05$, $^{**}p \leq 0.01$ (one-way ANOVA with Tukey's post hoc test).

Furthermore, PCB-95-mediated increases in RIPK1, RIPK3 and MLKL gene and protein expression were reversed by transfection of silencing for REST, thereby suggesting that by up-regulating REST expression PCB-95 treatment modulates transcription of necroptosis pathway genes. Bioinformatics analysis with the Jaspar database showed no REST binding, but did identify CREB binding sites, which may be important for down-regulating expression of these genes. Through REST, PCB-95 treatment induced reduction in levels of CREB and consequent increases in RIPK1, RIPK3 and MLKL expression. Moreover, REST silencing reversed PCB-induced reductions in CREB levels, whereas CREB overexpression in PCB-95-treated neurons blocked RIPK1, RIPK3 and MLKL increases. Together these results suggested that: (1) REST is a CREB repressor and (2) CREB is a transcriptional suppressor of RIPK1, RIPK3 and MLKL genes. Notably, in previous studies it has been showed that CREB positively regulates REST expression in small-cell lung cancer [33]. However, the finding that REST silencing reversed PCB-95-mediated reduction in CREB seems to suggest that in our experimental model REST is a regulator of CREB expression. Indeed, we found one CRE site in rat RIPK1, RIPK3 and MLKL genes (RIPK1-CRE, RIPK3-CRE and MLKL-CRE) located at −792/−771, −1013/−992 and −1081/−1060, respectively, from the TSS, which may act as molecular determinants involved in CREB-induced RIPK1, RIPK3 and MLKL regulation. Importantly, ChIP experiments revealed that PCB-95 induced a reduction in CREB binding to the RIPK1-CRE, RIPK3-CRE and MLKL-CRE sites, and this binding was sequence-specific as shown by luciferase experiments in neurons transfected with constructs containing the relevant CRE sites. To our knowledge, this is the first characterization of the relationship between PCB-95 exposure and CREB expression.

Together our results indicate that CREB-dependent reduction in RIPK1, RIPK3 and MLKL expression is induced by PCB-95 through increases in REST. Although CREB can act as a transcriptional gene activator [33] or transcriptional gene repressor [34], in this model it acts as a repressor of RIPK1, RIPK3 and MLKL genes. These results are consistent with a previous study demonstrating that CREB negatively regulates insulin-like growth factor 2 receptor gene expression in cardiomyoblasts [35]. Moreover, our findings support the well-known neuroprotective role of CREB in neurological disorders associated with cell death, such as stroke and epilepsy [36]. From our findings that the CREB rat promoter sequence lacks an RE1 binding site and that neither PCB-95 treatment nor siRNA mediated knockdown of REST expression affected CREB gene expression, we hypothesize that PCB-95-mediated effects are not due to the binding of REST to the CREB rat promoter sequence.

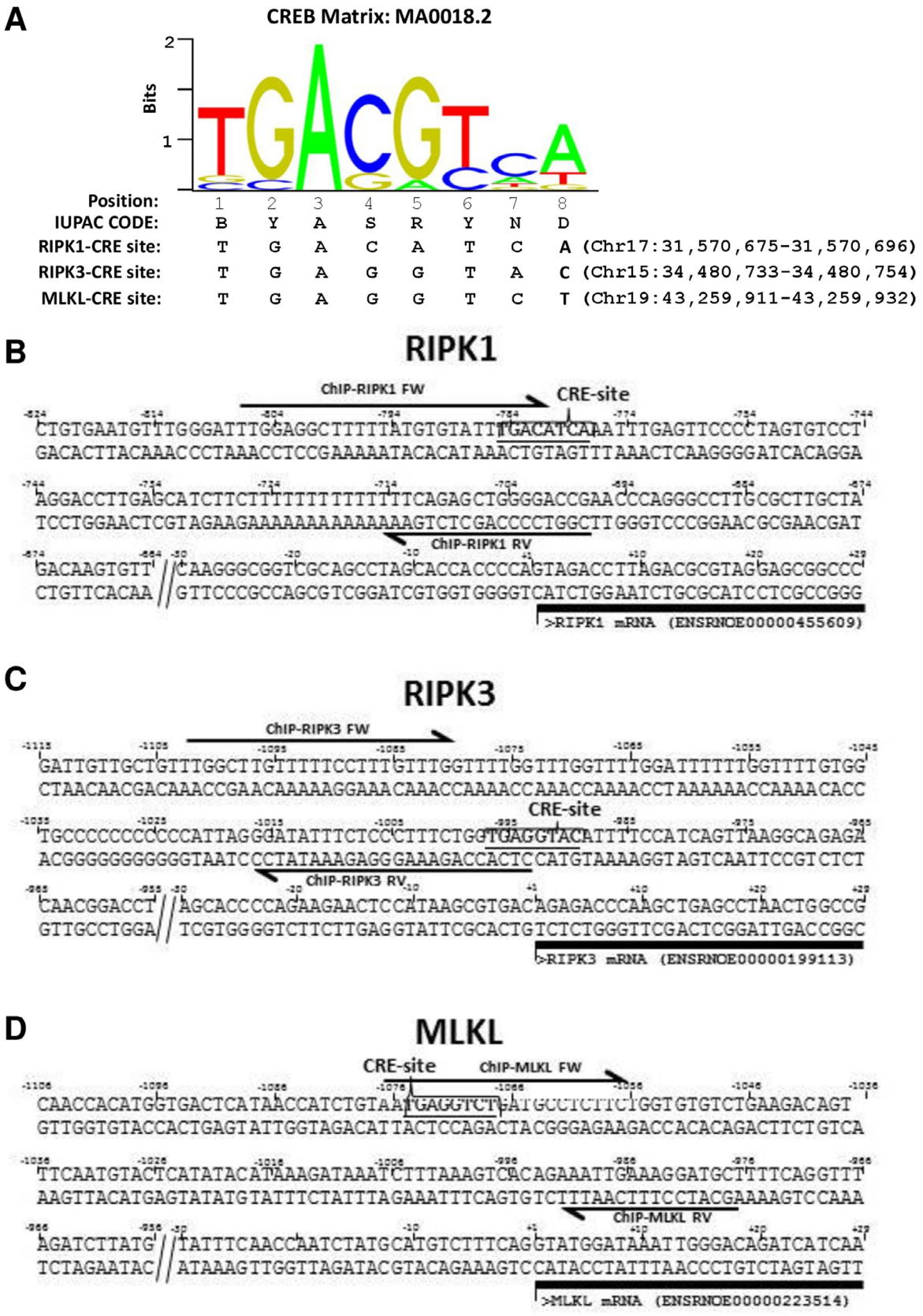

Fig. 5. Identification of putative CREB binding sites on RIPK1, RIPK3 and MLKL rat genes. (A) JASPAR matrix representation (MA0018.2) of the consensus CREB binding site on rat RIPK1 (RIPK1-CRE), RIPK3 (RIPK3-CRE) and MLKL (MLKL-CRE) genes. RIPK1-CRE site, RIPK3-CRE site and MLKL-CRE site are represented in IUPAC code. (B–D) Partial sequences of the genomic RIPK1, RIPK3 and MLKL regions upstream of the exon-1 containing the underlined predicted CREB binding sites.

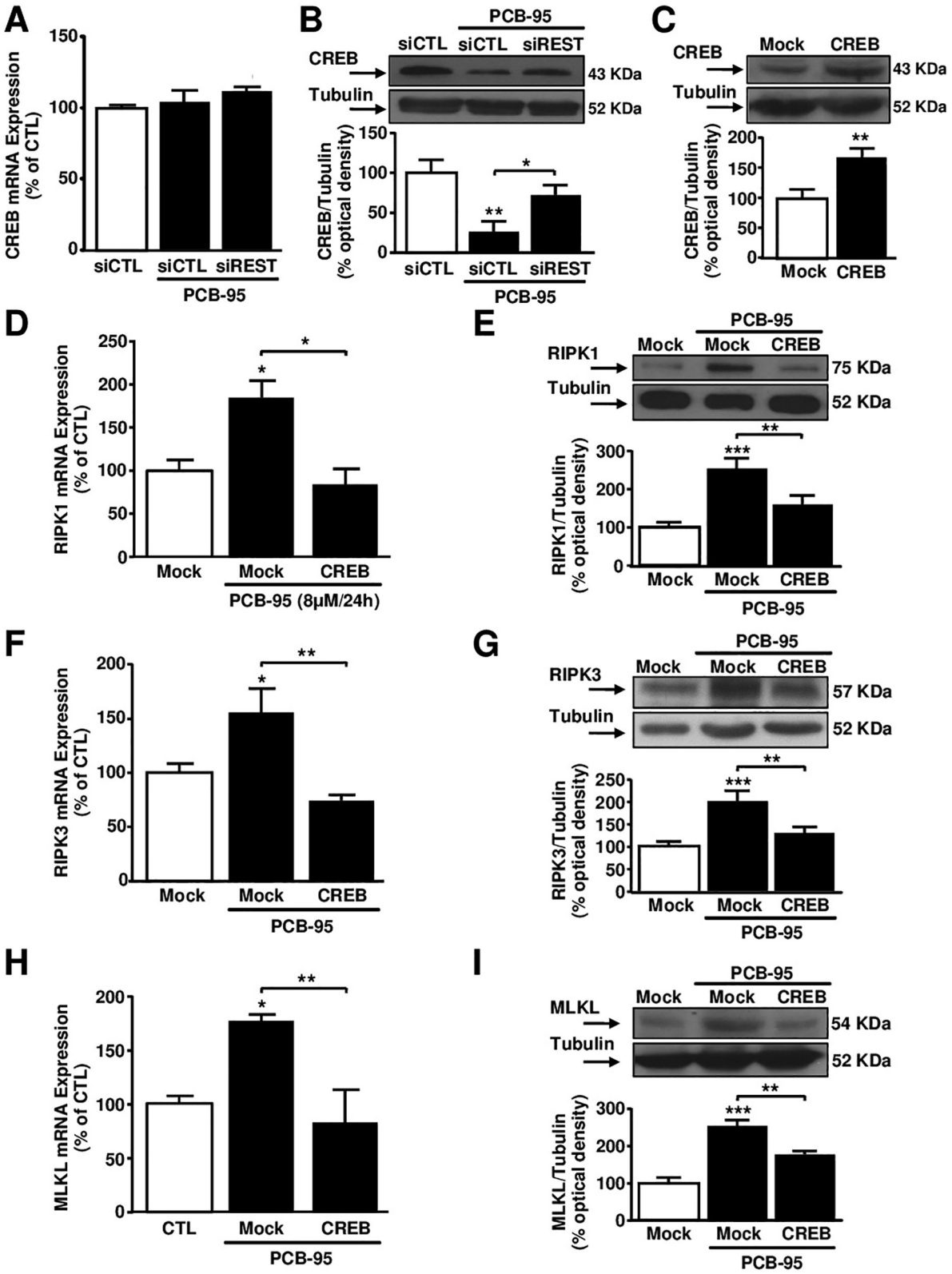

Fig. 6. REST by down-regulating CREB increases RIPK1, RIPK3, MLKL mRNA and protein expression in neurons treated with PCB-95. (A, B) qRT-PCR and Western blot analysis of CREB in cortical neurons treated with 8 μM of PCB-95 for 24 h and transfected with siCTL or siREST. Bars represent mean ± S.E.M. obtained from three independent experiments. Asterisk symbols on columns indicate differences between siCTL and siCTL + PCB-95. Asterisk symbols on brackets indicate differences between siCTL + PCB-95 and siREST + PCB-95. $^{*}p \leq 0.05$ and $^{**}p \leq 0.01$ (one-way ANOVA with Tukey's post hoc test). (C) Western blot of CREB in neurons transfected with an empty vector (Mock) or with a plasmid overexpressing CREB. Bars represent the mean ± S.E.M. obtained from three independent experiments. Asterisk symbols indicate differences between Mock and CREB. $^{**}p \leq 0.01$ (unpaired *t*-test). (D–I) qRT-PCR and Western blot of RIPK1, RIPK3, MLKL in cells transfected with Mock or CREB and treated with PCB-95. Bars represent the mean ± S.E.M. obtained from three independent experiments. Asterisk symbols on columns indicate differences between Mock and Mock + PCB-95. Asterisk symbols on brackets indicate differences between Mock + PCB-95 and CREB + PCB-95. $^{*}p \leq 0.05$, $^{**}p \leq 0.01$, $^{***}p \leq 0.001$ (one-way ANOVA with Tukey's post hoc test).

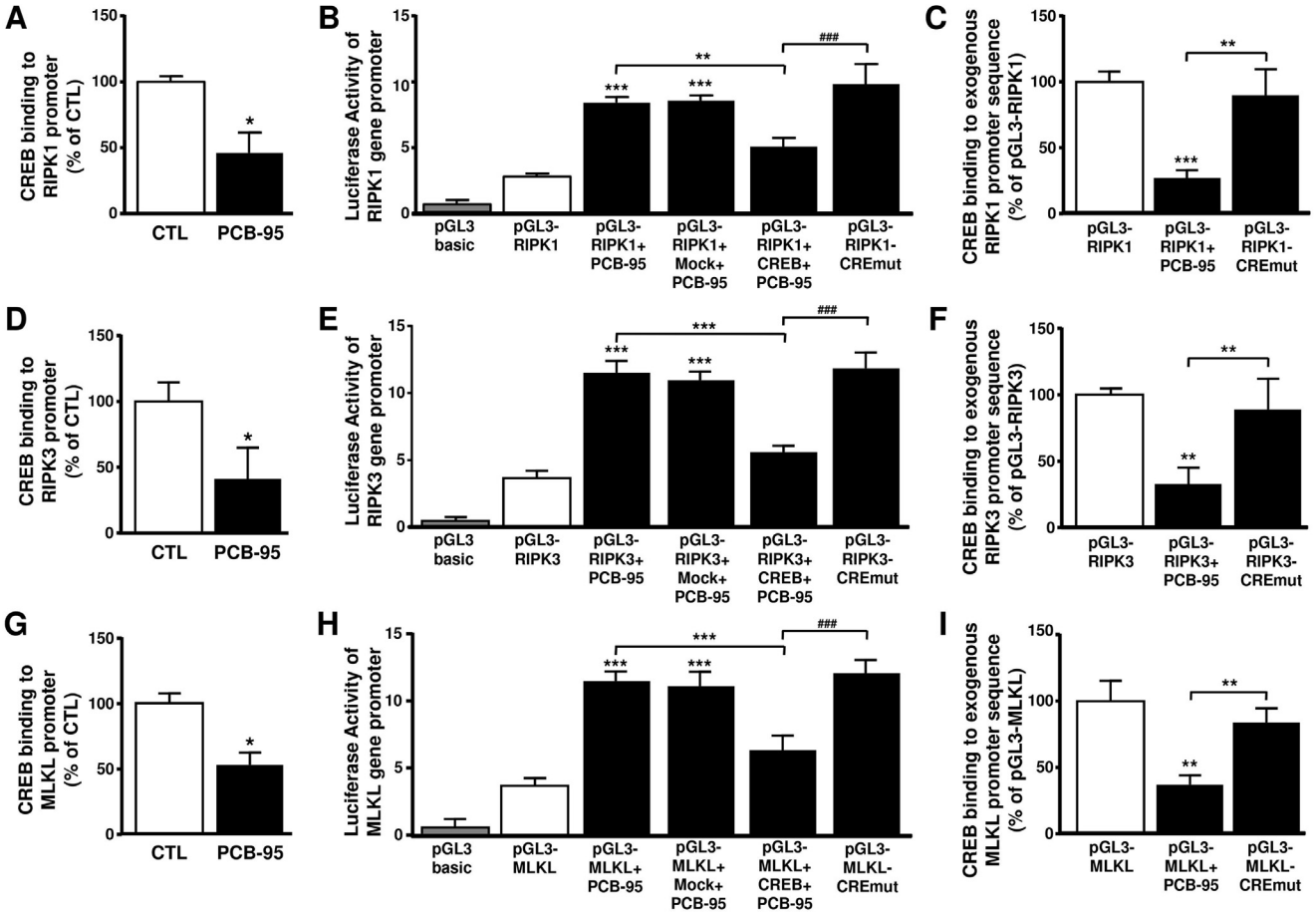

Fig. 7. CREB represses RIPK1, RIPK3 and MLKL genes by direct binding to a CRE site on their promoter regions. (A, D, G) ChIP with anti-CREB of the regions containing the CREB binding sites on the RIPK1, RIPK3 and MLKL gene promoters in PCB-95-treated neurons (8 μM/24 h). Bars represent the mean ± S.E.M. obtained from three independent experiments. $^{*}p \leq 0.05$ vs CTL (unpaired *t*-test). (B) Luciferase assay in cortical neurons under the following experimental conditions: (1) pGL3-basic, (2) pGL3-RIPK1, (3) pGL3-RIPK1 + PCB-95, (4) pGL3-RIPK1 + Mock + PCB-95, (5) pGL3-RIPK1 + CREB + PCB-95, (6) pGL3-RIPK1-CREmut constructs. Bars represent the mean ± S.E.M. obtained from three independent experiments. Asterisk symbols on columns indicate differences vs pGL3-RIPK1. Asterisk symbols on brackets indicate differences between pGL3-RIPK1 + PCB-95 and pGL3-RIPK1 + CREB + PCB-95. Hashtag symbols on brackets indicate differences between pGL3-RIPK1 + CREB + PCB-95 and pGL3-RIPK1-CREmut. $^{**}p \leq 0.01$ and $^{***}p \leq 0.001$, $^{\#\#\#}p \leq 0.001$ (one-way ANOVA with Tukey's post hoc test). (E) Luciferase assay in cortical neurons under the following experimental conditions: (1) pGL3-basic, (2) pGL3-RIPK3, (3) pGL3-RIPK3 + PCB-95, (4) pGL3-RIPK3 + Mock + PCB-95, (5) pGL3-RIPK3 + CREB + PCB-95,(6) pGL3-RIPK3-CREmut constructs. Bars represent the mean ± S.E.M. obtained from three independent experiments. Asterisk symbols on columns indicate differences vs pGL3-RIPK3. Asterisk symbols on brackets indicate differences between pGL3-RIPK3 + PCB-95 and pGL3-RIPK3 + CREB + PCB-95. Hashtag symbols on brackets indicate differences between pGL3-RIPK3 + CREB + PCB-95 and pGL3-RIPK3-CREmut. $^{***}p \leq 0.001$, $^{\#\#\#}p \leq 0.001$ (one-way ANOVA with Tukey's post hoc test). (H) Luciferase assay in cortical neurons under the following experimental conditions: (1) pGL3-basic, (2) pGL3-MLKL, (3) pGL3-MLKL + PCB-95, (4) pGL3-MLKL + Mock + PCB-95, (5) pGL3-MLKL + CREB + PCB-95, (6) pGL3-MLKL-CREmut constructs. Bars represent the mean ± S.E.M. obtained from three independent experiments. Asterisk symbols on columns indicate differences vs pGL3-MLKL. Asterisk symbols on brackets indicate differences between pGL3-MLKL + PCB-95 and pGL3-MLKL + CREB + PCB-95. Hashtag symbols on brackets indicate differences between pGL3-MLKL + CREB + PCB-95 and pGL3-MLKL-CREmut. $^{***}p \leq 0.001$, $^{\#\#\#}p \leq 0.001$ (one-way ANOVA with Tukey's post hoc test). (C, F, I) Chromatin was immunoprecipitated with CREB antibody from SH-SY5Y cells transiently transfected with: (C) pGL3-RIPK1 and pGL3-RIPK1-CREmut, (F) pGL3-RIPK3 and pGL3-RIPK3-CREmut, (I) pGL3-MLKL and pGL3-MLKL-CREmut and therefore exposed to PCB-95 (8 μM/24 h). Bars represent the mean ± S.E.M. obtained from three independent experiments. Asterisk symbols on columns indicate differences vs pGL3-RIPK1 (C), pGL3-RIPK3 (F) and pGL3-MLKL (I). Asterisk symbols on brackets indicate differences vs pGL3-RIPK1 + PCB-95 (C), pGL3-RIPK3 + PCB-95 (F) or pGL3-MLKL + PCB-95 (I). $^{**}p \leq 0.01$, $^{***}p \leq 0.001$ (one-way ANOVA with Tukey's post hoc test).

To our knowledge, this is the first report showing that PCB-95 can induce necroptosis in neurons and is in accordance with our previous study demonstrating that neurons exposed to 8 μM PCB-95 for 24 h showed no caspase-3 activation, that is typical of apoptosis, and supports the involvement of programmed necrosis [11].

Necroptosis is a relevant mechanism of cell death in *in vitro* and *in vivo* models of neurological diseases such as ALS, Huntington's disease, Parkinson's disease [37], stroke [16] and MS [18]. Notably, in models of all these diseases, cell survival was increased and necroptosis was reduced by treatment with the RIPK1-specific inhibitor Nec-1. Here we also observed that Nec-1 dose-dependently reduced PCB-95 induced neuronal death, with 10 MM having the maximum inhibitor effect on PCB-95-induced neurotoxicity. Additionally, we found that RIPK1, RIPK3 and MLKL knockdown reverted the neurotoxic effect of PCB-95, suggesting involvement of these proteins in neuronal necroptosis, which is similar to previous findings in other cell systems such as the kidney, where necroptosis is a major mechanism of proximal tubular cell death in cisplatin-induced nephrotoxic acute kidney injury [38]. Furthermore, in our system we cannot exclude the possibility that other concentrations or treatment times for PCB-95 could activate other types of cell death such as apoptosis or autophagy. In addition, we did not test the effect of the MLKL inhibitor necrosulfonamide on PCB-95-induced cell death in primary rat cortical neurons because this drug is specific for the human isoform [39].

PCB-95 exposure has also been identified as a probable environmental risk factor for neurodevelopmental disorders such as autism. A recent study by Dunaway et al. analyzed human brain tissue complemented with experimental neuronal cell culture

models to demonstrate a cumulative effect of large chromosome duplications and PCB-95 exposure on genes that have roles in neuronal synapses, transcriptional regulation, and signal transduction pathways [40].

Collectively, our results indicate that necroptotic-dependent cell death induced by PCB-95 treatment in rat cortical neurons depends on increases in REST expression that elicit: (1) reduced caspase-8 gene and protein expression directly induced by REST binding to a specific rE-1 site present in the caspase-8 promoter sequence and (2) increased RIPK1, RIPK3, and MLKL gene and protein expression via a reduction in CREB binding to putative promoter sequences. Furthermore, the necroptotic death pathway mediated by PCB-95 exposure could underlie the damaging effect of REST that is associated with stroke [16,22,41–43]. In fact, both REST and activation of necroptosis are associated with physiopathological mechanisms of brain ischemia. Drugs that inhibit necroptosis could be a new therapeutic strategy for many neurological diseases associated with PCB exposure or where the transcription factor REST is overexpressed.

Acknowledgements

This work was supported by the following grants: PON03PE_00146_1 by MIUR to Lucio Annunziato, POR Campania FESR Q8 2007–2013 to OCKEY (B25C1300028007) to Gianfranco Di Renzo and PRIN 2015 (2015 BEX2BR) by MIUR and FRA 2016 from DST University of Sannio both to Luigi Formisano.

References

[1] E. Eljarrat, D. Barceló, Priority lists for persistent organic pollutants and emerging contaminants based on their relative toxic potency in environmental samples, TrAC Trends Anal. Chem. 22 (10) (2003) 655–665.
[2] A. Aguilar, A. Borrell, DDT and PCB reduction in the western Mediterranean from 1987 to 2002, as shown by levels in striped dolphins (*Stenella coeruleoalba*), Mar. Environ. Res. 59 (4) (2005) 391–404.
[3] D. Carpenter, Polychlorinated biphenyls (PCBs): routes of exposure and effects on human health, Rev. Environ. Health 21 (1) (2006) 1–23.
[4] M. Yegambaram, B. Manivannan, T.G. Beach, R.U. Halden, Role of environmental contaminants in the etiology of Alzheimer's disease: a review, Curr. Alzheimer Res. 12 (2) (2015) 116–146.
[5] J.M. Hatcher-Martin, M. Gearing, K. Steenland, A.I. Levey, G.W. Miller, K.D. Pennell, Association between polychlorinated biphenyls and Parkinson's disease neuropathology, Neurotoxicology 33 (5) (2012) 1298–1304.
[6] F.C. Su, S.A. Goutman, S. Chernyak, B. Mukherjee, B.C. Callaghan, S. Batterman, E.L. Feldman, Association of environmental toxins with amyotrophic lateral sclerosis, JAMA Neurol. 73 (7) (2016) 803–811.
[7] J.P. Giesy, K. Kannan, Dioxin-like and non-dioxin-like toxic effects of polychlorinated biphenyls (PCBs): implications for risk assessment, Crit. Rev. Toxicol. 28 (6) (1998) 511–569.
[8] J.Y. Lee, J.W. Kim, S.D. Cho, Y.H. Kim, K.J. Choi, W.H. Joo, Y.K. Cho, J.Y. Moon, Protective effect of ginseng extract against apoptotic cell death induced by 2,2',5,5'-tetrachlorobiphenyl in neuronal SK-N-MC cells, Life Sci. 75 (13) (2004) 1621–1634.
[9] J.A. Sanchez-Alonso, P. Lopez-Aparicio, M.N. Recio, M.A. Perez-Albarsanz, Apoptosis-mediated neurotoxic potential of a planar (PCB 77) and a nonplanar (PCB 153) polychlorinated biphenyl congeners in neuronal cell cultures, Toxicol. Lett. 144 (3) (2003) 337–349.
[10] S.M. Dickerson, E. Guevara, M.J. Woller, A.C. Gore, Cell death mechanisms in GT1-7 GnRH cells exposed to polychlorinated biphenyls PCB74, PCB118, and PCB153, Toxicol. Appl. Pharmacol. 237 (2) (2009) 237–245.
[11] N. Guida, G. Laudati, S. Anzilotti, A. Secondo, P. Montuori, G. Di Renzo, L.M. Canzoniero, L. Formisano, Resveratrol via sirtuin-1 downregulates RE1-silencing transcription factor (REST) expression preventing PCB-95-induced neuronal cell death, Toxicol. Appl. Pharmacol. 288 (3) (2015) 387–398.
[12] L. Formisano, N. Guida, S. Cocco, A. Secondo, R. Sirabella, L. Ulianich, F. Paturzo, G. Di Renzo, L.M. Canzoniero, The repressor element 1-silencing transcription factor is a novel molecular target for the neurotoxic effect of the polychlorinated biphenyl mixture aroclor 1254 in neuroblastoma SH-SY5Y cells, J. Pharmacol. Exp. Ther. 338 (3) (2011) 997–1003.
[13] Y. Zhao, M. Zhu, Y. Yu, L. Qiu, Y. Zhang, L. He, J. Zhang, Brain REST/NRSF is not only a silent repressor but also an active protector, Mol. Neurobiol. 54 (1) (2017) 541–550.
[14] L. Formisano, N. Guida, G. Laudati, L. Mascolo, G. Di Renzo, L.M. Canzoniero, MS-275 Inhibits aroclor 1254-induced SH-SY5Y neuronal cell toxicity by preventing the formation of the HDAC3/REST complex on the synapsin-1 promoter, J. Pharmacol. Exp. Ther. 352 (2) (2015) 236–243.
[15] L. Formisano, N. Guida, G. Laudati, F. Boscia, A. Esposito, A. Secondo, G. Di Renzo, L.M. Canzoniero, Extracellular signal-related kinase 2/specificity protein 1/specificity protein 3/repressor element-1 silencing transcription factor pathway is involved in Aroclor 1254-induced toxicity in SH-SY5Y neuronal cells, J. Neurosci. Res. 93 (1) (2015) 167–177.
[16] M. Vieira, J. Fernandes, L. Carreto, B. Anuncibay-Soto, M. Santos, J. Han, A. Fernandez-Lopez, C.B. Duarte, A.L. Carvalho, A.E. Santos, Ischemic insults induce necroptotic cell death in hippocampal neurons through the up-regulation of endogenous RIP3, Neurobiol. Dis. 68 (2014) 26–36.
[17] Y. Ito, D. Ofengeim, A. Najafov, S. Das, S. Saberi, Y. Li, J. Hitomi, H. Zhu, H. Chen, L. Mayo, J. Geng, P. Amin, J.P. DeWitt, A.K. Mookhtiar, M. Florez, A.T. Ouchida, J. B. Fan, M. Pasparakis, M.A. Kelliher, J. Ravits, J. Yuan, RIPK1 mediates axonal degeneration by promoting inflammation and necroptosis in ALS, Science 353 (6299) (2016) 603–608.
[18] D. Ofengeim, Y. Ito, A. Najafov, Y. Zhang, B. Shan, J.P. DeWitt, J. Ye, X. Zhang, A. Chang, H. Vakifahmetoglu-Norberg, J. Geng, B. Py, W. Zhou, P. Amin, J. Berlink Lima, C. Qi, Q. Yu, B. Trapp, J. Yuan, Activation of necroptosis in multiple sclerosis, Cell Rep. 10 (11) (2015) 1836–1849.
[19] H. Zhao, T. Jaffer, S. Eguchi, Z. Wang, A. Linkermann, D. Ma, Role of necroptosis in the pathogenesis of solid organ injury, Cell Death Dis. 6 (2015) e1975.
[20] J. Yuan, A. Najafov, B.F. Py, Roles of caspases in necrotic cell death, Cell 167 (7) (2016) 1693–1704.
[21] A. Linkermann, D.R. Green, Necroptosis, N. Engl. J. Med. 370 (5) (2014) 455–465.
[22] L. Formisano, N. Guida, V. Valsecchi, M. Cantile, O. Cuomo, A. Vinciguerra, G. Laudati, G. Pignataro, R. Sirabella, G. Di Renzo, L. Annunziato, Sp3/REST/HDAC1/HDAC2 complex represses and Sp1/HIF-1/p300 complex activates ncx1 gene transcription brain ischemia and in ischemic brain preconditioning, by epigenetic mechanism, J. Neurosci. 35 (19) (2015) 7332–7348.
[23] N. Guida, G. Laudati, L. Mascolo, V. Valsecchi, R. Sirabella, C. Selleri, G. Di Renzo, L.M. Canzoniero, L. Formisano, p38/Sp1/Sp4/HDAC4/BDNF axis is a novel molecular pathway of the neurotoxic effect of the methylmercury, Front. Neurosci. 11 (2017) 8.
[24] W.W. Wasserman, A. Sandelin, Applied bioinformatics for the identification of regulatory elements, Nat. Rev. Genet. 5 (4) (2004) 276–287.
[25] G.A. Gonzalez, M.R. Montminy, Cyclic AMP stimulates somatostatin gene transcription by phosphorylation of CREB at serine 133, Cell 59 (4) (1989) 675–680.
[26] N. Guida, G. Laudati, L. Mascolo, O. Cuomo, S. Anzilotti, R. Sirabella, M. Santopaolo, M. Galgani, P. Montuori, G. Di Renzo, L.M. Canzoniero, L. Formisano, MC1568 inhibits thimerosal-induced apoptotic cell death by preventing HDAC4 up-regulation in neuronal cells and in rat prefrontal cortex, Toxicol. Sci. 154 (2) (2016) 227–240.
[27] N. Guida, G. Laudati, M. Galgani, M. Santopaolo, P. Montuori, M. Triassi, G. Di Renzo, L.M. Canzoniero, L. Formisano, Histone deacetylase 4 promotes ubiquitin-dependent proteasomal degradation of Sp3 in SH-SY5Y cells treated with di(2-ethylhexyl)phthalate (DEHP), determining neuronal death, Toxicol. Appl. Pharmacol. 280 (1) (2014) 190–198.
[28] N. Guida, G. Laudati, S. Anzilotti, R. Sirabella, O. Cuomo, P. Brancaccio, M. Santopaolo, M. Galgani, P. Montuori, G. Di Renzo, L.M. Canzoniero, L. Formisano, Methylmercury upregulates RE-1 silencing transcription factor (REST) in SH-SY5Y cells and mouse cerebellum, Neurotoxicology 52 (2015) 89–97.
[29] F.A. Iannotti, V. Barrese, L. Formisano, F. Miceli, M. Taglialatela, Specification of skeletal muscle differentiation by repressor element-1 silencing transcription factor (REST)-regulated Kv7.4 potassium channels, Mol. Biol. Cell 24 (3) (2013) 274–284.
[30] L. Sun, H. Wang, Z. Wang, S. He, S. Chen, D. Liao, L. Wang, J. Yan, W. Liu, X. Lei, X. Wang, Mixed lineage kinase domain-like protein mediates necrosis signaling downstream of RIP3 kinase, Cell 148 (1–2) (2012) 213–227.
[31] J.C. Bryne, E. Valen, M.H. Tang, T. Marstrand, O. Winther, I. da Piedade, A. Krogh, B. Lenhard, A. Sandelin, JASPAR, the open access database of transcription factor-binding profiles: new content and tools in the 2008 update, Nucleic Acids Res 36 (Database issue) (2008) D102–D106.
[32] A. Lesiak, M. Zhu, H. Chen, S.M. Appleyard, S. Impey, P.J. Lein, G.A. Wayman, The environmental neurotoxicant PCB 95 promotes synaptogenesis via ryanodine receptor-dependent miR132 upregulation, J. Neurosci. 34 (3) (2014) 717–725.
[33] A. Kreisler, P.L. Strissel, R. Strick, S.B. Neumann, U. Schumacher, C.M. Becker, Regulation of the NRSF/REST gene by methylation and CREB affects the cellular phenotype of small-cell lung cancer, Oncogene 29 (43) (2010) 5828–5838.
[34] A.J. Shaywitz, M.E. Greenberg, CREB: a stimulus-induced transcription factor activated by a diverse array of extracellular signals, Annu. Rev. Biochem. 68 (1999) 821–861.
[35] W.K. Chen, W.W. Kuo, D.J. Hsieh, H.N. Chang, P.Y. Pai, K.H. Lin, L.F. Pan, T.J. Ho, V.P. Viswanadha, C.Y. Huang, CREB negatively regulates IGF2R gene expression and downstream pathways to inhibit hypoxia-induced h9c2 cardiomyoblast cell death, Int. J. Mol. Sci. 16 (11) (2015) 27921–27930.
[36] M.R. Walton, I. Dragunow, Is CREB a key to neuronal survival? Trends Neurosci. 23 (2) (2000) 48–53.
[37] J.R. Morrice, C.Y. Gregory-Evans, C.A. Shaw, Necroptosis in amyotrophic lateral sclerosis and other neurological disorders, Biochim. Biophys. Acta 1863 (2) (2017) 347–353.
[38] Y. Xu, H. Ma, J. Shao, J. Wu, L. Zhou, Z. Zhang, Y. Wang, Z. Huang, J. Ren, S. Liu, X. Chen, J. Han, A role for tubular necroptosis in cisplatin-induced AKI, J. Am. Soc. Nephrol. 26 (11) (2015) 2647–2658.

[39] T. Vanden Berghe, A. Linkermann, S. Jouan-Lanhouet, H. Walczak, P. Vandenabeele, Regulated necrosis: the expanding network of non-apoptotic cell death pathways, Nat. Rev. Mol. Cell Biol. 15 (2) (2014) 135–147.
[40] K.W. Dunaway, M.S. Islam, R.L. Coulson, S.J. Lopez, A. Vogel Ciernia, R.G. Chu, D. H. Yasui, I.N. Pessah, P. Lott, C. Mordaunt, M. Meguro-Horike, S.I. Horike, I. Korf, J.M. LaSalle, Cumulative impact of polychlorinated biphenyl and large chromosomal duplications on DNA methylation chromatin, and expression of autism candidate genes, Cell Rep. 17 (11) (2016) 3035–3048.
[41] L. Formisano, N. Guida, V. Valsecchi, G. Pignataro, A. Vinciguerra, A. Pannaccione, A. Secondo, F. Boscia, P. Molinaro, M.J. Sisalli, R. Sirabella, A. Casamassa, L.M. Canzoniero, G. Di Renzo, L. Annunziato, NCX1 is a new rest target gene: role in cerebral ischemia, Neurobiol. Dis. 50 (2013) 76–85.
[42] L. Formisano, K. Noh, T. Miyawaki, T. Mashiko, M. Bennett, R. Zukin, Ischemic insults promote epigenetic reprogramming of mu opioid receptor expression in hippocampal neurons, Proc. Natl. Acad. Sci. U. S. A. 104 (10) (2007) 4170–4175.
[43] J.Y. Hwang, K.A. Aromolaran, R.S. Zukin, The emerging field of epigenetics in neurodegeneration and neuroprotection, Nat. Rev.Neurosci 18 (6) (2017) 347–361.